South East Asian J. of Mathematics and Mathematical Sciences
Vol. 20, No. 2 (2024), pp. 213-234

DOI: 10.56827/SEAJMMS.2024.2002.17 **ISSN (Online): 2582-0850**

ISSN (Print): 0972-7752

EFFECTS OF CONTACT TRACING AND QUARANTINE STRATEGIES IN REDUCTION OF SPREAD OF AN EPIDEMIC

Pradeep Kumar Yadav and Vijai Shanker Verma

Department of Mathematics and Statistics,
Deen Dayal Upadhyaya Gorakhpur University,
Gorakhpur - 273009, Uttar Pradesh, INDIA

E-mail : drvsverma01@gmail.com

(**Received:** *Nov. 28, 2023* **Accepted:** *Jul. 10, 2024* **Published:** *Aug. 30, 2024)*

Abstract: In this paper, a compartmental model is proposed to study the effects of contact tracing and quarantine strategies to reduce the spread of an epidemic. The basic properties of the model are discussed and the equilibrium points are computed. The basic reproduction number is calculated by using the next-generation matrix approach. After calculating the basic reproduction number R_0, the stability analysis of the model is carried out. Sensitivity and bifurcation analyses are also performed. Numerical simulations are performed to observe the effects of contact tracing and quarantine strategies in reducing the spread of the epidemic. The results are displayed graphically to justify the analytical findings. The disease-free equilibrium point is shown to be locally asymptotically stable when $R_0 < 1$ and unstable when $R_0 > 1$ and the endemic equilibrium point is shown to be locally asymptotically stable.

Keywords and Phrases: High and low infection risks, equilibrium points, stability analysis, bifurcation analysis and numerical simulations.

2020 Mathematics Subject Classification: 34D20, 34D23, 34D08.

1. Introduction

Mathematical modelling has become very important tool in epidemiology to understand the dynamics of infectious diseases and predict the consequences of introducing public health interventions to control the spread of diseases. Among all

intervention policies, vaccination is considered as the most useful and cost-effective strategy to control the spread of diseases. Vaccination is the administration of antigenic material to stimulate the immune system of an individual to develop adaptive immunity to a disease. Vaccination is useful in tackling many diseases such as COVID-19, measles, rubella, tetanus, hepatitis B, influenza, etc. However, vaccination does not necessarily imply life-long immunity for vaccinated persons [5, 21, 26]. There are some infectious diseases such as tetanus, diphtheria, hepatitis B, influenza, etc. which all have temporary vaccine-induced immunity. For influenza, the vaccine induces immunity that lasts only three to six months. Furthermore, it is practically impossible to vaccinate all the susceptible individuals in a given community, especially in those countries where vaccines are not easily available or affordable. Hence, a framework that would predict the optimal vaccine coverage level is a primary goal of health administrators and policy makers [2, 4, 6-9, 11, 12, 15, 20].

Besides vaccination [7, 9, 12, 15], there are many more preventive measures, which have been used to reduce the spread of various infectious diseases. These preventive measures include contact tracing, quarantine, prevention and treatment, etc. Contact tracing [1, 11] followed by treatment or quarantine is a key control measure in the battle against infectious diseases. In epidemiology, [20] contact tracing means the identification and diagnosis of an infected person. Aparicio and Hernandez [2] studied the effect of contact tracing in analyzing tuberculosis(TB).

Another preventive measure quarantine has been used to reduce the spread of various infectious diseases for a long time. Quarantine is defined as the forced isolation or stoppage of interaction with others. Quarantine has been used to reduce the spread of many human diseases such as leprosy, plague, smallpox, typhus, yellow fever, influenza, COVID-19, etc. It has also been used for animal diseases such as psittacosis and rabies. Chinviriyasit et al. [8] studied the global stability of a model for the transmission dynamics of infectious diseases with a new class of quarantined individuals, who have been removed and isolated either voluntarily or coercively from the infectious class. Hethcote et al. [14] studied the effects of quarantine in six endemic models for infectious diseases. They have found threshold equilibria and their stability for SIQS and SIQR epidemiological models with three kinds of incidence. Hu et al. [16] analyzed two epidemic models with constant immigration and quarantine. Zaman et al. [25] have discussed an SIR epidemic model with three population classes: susceptible population, infected population, and recovered population.

Goudiaby et al. [13] have investigated optimal control strategies of COVID-19 and TB dynamics by incorporating five control measures. An SVIQR epidemic

model for COVID-19 is studied by Verma et al. [22] who suggested that the disease will eventually die out if the control measures are implemented above a specified level for a sustained period. A mathematical analysis of the SVEIQR model for COVID-19 is presented by Kunwar and Verma [18] in which the impact of different degrees of control interventions is ascertained with the numerical simulation of the model. Fei Wu et al. [24] have given a model that combines compartmental and individual-based simulations, resulting in a delay differential equation model with unique quarantine functions. Biala et al. [3] have investigated the efficacy of contact tracing (CT) in reducing the spread of COVID-19. They developed a compartmental model to assess its impact on mitigating the virus and describe its effect on the reproduction number (R_0). Pozo-Martin et al. [19] have shown that contact tracing is a key non-pharmaceutical intervention in the fight against COVID-19. Factors influencing its efficacy include contact proportion, tracing speed, methods used, types of contacts traced, and setting. While observational studies recognized its impact, limitations like insufficient implementation details exist. Effective policies include manual and digital tracing with high coverage, integration with other interventions, and timely actions. Izadi and Waezizadeh [17] have proposed a non-linear mathematical model with eight compartments to study the impact of vaccination on COVID-19. Waezizadeh et al. [26] have formulated a novel mathematical model for COVID-19 with reinfection. They performed the numerical simulation to analyze the solution.

In view of the above studies, a compartmental model is proposed to study the impact of contact tracing and quarantine strategies in reducing the spread of an epidemic. The saturation incidence rate of infection is also included in the model because of its large population size.

2. Model Formulation

In the model, we have divided the total population into five compartments: S_1-susceptible with high infection risk (who are prone to getting highly infected from infectives),S_2-susceptible with low infection risk (who are prone to getting less infected from infectives), I-infectives(who have the infection and are capable of infecting others actively), Q-quarantined (who are infected and forced to stop interaction with others and forced to live in isolation), and R-recovered (who are immune to infection after treatment or self-protection). The detailed description of model parameters is given in Table 1. We have also used saturation incidence rate of infection to include the effect of force of infection in the model.

It is assumed that the high-risk susceptible population enters into the system at the rate $(1-\psi)$A and the low-risk susceptible population enters into the system at the rate ψA, where ψ is the immunity rate of low-risk population and A is the

recruitment rate. β is the transmission coefficient of infection and p is the rate of reduction in transmission of infection for low-risk susceptible population due to its immunity towards infection. People with weakened immune systems might not develop full immunity after infection and might be more likely to be infected with the virus more than once. It is assumed that the recovered population again enters into the susceptible population but with a low-risk of infection at the rate θ. We assume that only a fraction of the total of newly infected contacts are elucidated and that those individuals are quarantined [1]. This fraction moves directly from the susceptible class to the quarantined class while rest of them move to the infective class. We have also taken k as the rate at which newly infected people are detected by the system through contact tracing. Population in the infective compartment requiring special diagnosis and treatment are also isolated and moved to the quarantined class Q(t) at the rate σ. We have assumed δ_1 and δ_2 respectively as the recovery rate constants of population in infective and quarantined classes. The schematic representation of the model is given in Figure 1.

Keeping the above assumptions into consideration, the proposed model is described by the following system of differential equations:

$$\left.\begin{aligned}
\frac{dS_1}{dt} &= (1-\psi)A - \frac{\beta S_1 I}{(1+\alpha I)} - \mu S_1, \\
\frac{dS_2}{dt} &= \psi A - \frac{p\beta S_2 I}{(1+\alpha I)} - \mu S_2 + \theta R, \\
\frac{dI}{dt} &= \frac{(1-k)\beta(S_1+pS_2)I}{(1+\alpha I)} - (\mu+\delta_1+\sigma)I, \\
\frac{dQ}{dt} &= \frac{k\beta(S_1+pS_2)I}{(1+\alpha I)} - (\mu+\delta_2)Q + \sigma I, \\
\frac{dR}{dt} &= \delta_1 I + \delta_2 Q - \mu R - \theta R.
\end{aligned}\right\} \tag{1}$$

with following initial conditions:

$$S_1(0) \geq 0, S_2(0) \geq 0, I(0) > 0, Q(0) \geq 0, R(0) \geq 0 \tag{2}$$

Also, we have $N(t) = S_1(t) + S_2(t) + I(t) + Q(t) + R(t)$.

Table 1: **Description of Model Parameters**

Parameter	**Description**
A	Recruitment rate
ψ	Immunity rate of low-risk population
β	Transmission coefficient of infection
p	Rate of reduction in transmission of infection for low risk susceptible population
k	Rate of detection of newly infected population through contact tracing
θ	Rate of conversion of recovered population re-entering into low-risk susceptible population
σ	Rate of movement of infected population to the quarantine population
δ_1	Recovery rate of infected population
δ_2	Recovery rate of quarantined population
α	Saturation incidence rate of infection
μ	Natural mortality rate

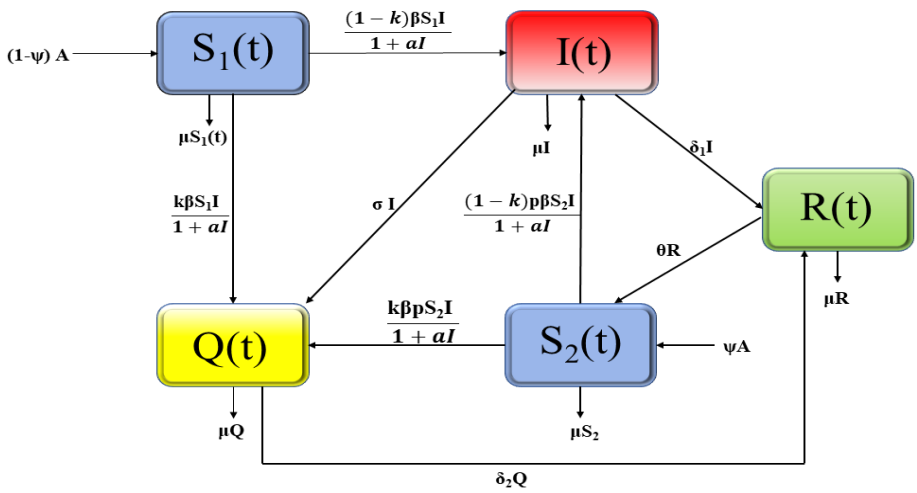

Figure 1: Compartmental Flow Diagram of the Proposed Model

3. Model Analysis and Basic Properties

We analyse the proposed model by including the following basic properties:

3.1. Non-negativity of the Model

Non-negativity conditions are necessary to show that all the state variables remain non-negative for $t \geq 0$ or every solution of the system remains positive for all $t \geq 0$.Thus, we have the following Lemma:

Lemma 1. *Under the initial conditions given by (2), every solution* (S_1, S_2, I, Q, R) *of the system (1) remains non-negative for all* $t \geq 0$.

Proof. From the system of eqns.(1) and (2), we have

$$\frac{dS_1}{dt}\Big|_{S_1=0} = (1-\psi)A \geq 0, \tag{3}$$

$$\frac{dS_2}{dt}\Big|_{S_2=0} = \psi A + \theta R \geq 0, \tag{4}$$

$$\frac{dI}{dt}\Big|_{I=0} = 0, \tag{5}$$

$$\frac{dQ}{dt}\Big|_{Q=0} = \frac{k\beta(S_1 + pS_2)I}{(1+\alpha I)} + \sigma I \geq 0, \tag{6}$$

$$\frac{dR}{dt}\Big|_{R=0} = \delta_1 I + \delta_2 Q \geq 0. \tag{7}$$

Thus, we conclude that every solution (S_1, S_2, I, Q, R) of the system (1) under the initial conditions (2) is non-negative for all $t \geq 0$.

3.2. Boundedness of the Model

Boundedness refers to the natural limits to the endless growth of an infected population as a result of numerous constraints such as preventative practices developed by the population to protect themselves from contracting the disease under consideration. We demonstrate that the solutions to the system (1) are bounded. Thus, we prove the following Lemma:

Lemma 2. *The set* $\Omega = \{(S_1, S_2, I, Q, R) : 0 < S_1 + S_2 + I + Q + R \leq N\}$ *is bounded for the system (1) with non-negative initial conditions (2) for all solutions initiating in the positive octant.*

Proof. Adding all the five equations of the system (1), and using the relation $N = S_1 + S_2 + I + Q + R$, we have

$$\frac{dN}{dt} = A - \mu N \tag{8}$$

Solving the above eqn.(8), we get

$$N = \frac{A}{\mu} + (N_0 - \frac{A}{\mu})e^{-\mu t} \tag{9}$$

Now, if $0 \leq N(0) \leq \frac{A}{\mu}$, then $lim\sup_{t\to\infty} N(t) \leq \frac{A}{\mu}$. Thus, we have

$$0 < N \leq \frac{A}{\mu} \tag{10}$$

Therefore, the set Ω=$\{(S_1, S_2, I, Q, R) : 0 \leq S_1 + S_2 + I + Q + R \leq N\}$ is bounded for the system (1) and all the solutions of the model enter in the set Ω. Thus, our proposed model is well-defined biologically and mathematically.

3.3. Basic Reproduction Number

The basic reproduction number R_0 is a dimensionless quantity that is essential in the analysis of any epidemiological model [10]. If the disease-free equilibrium of the given system exists, it can be determined analytically. To determine the basic reproduction number, we apply the next-generation matrix approach described by Driesseche and Watmough. For the system (1), the disease-free equilibrium point is computed as $E_0\left(\frac{(1-\psi)A}{\mu}, \frac{\psi A}{\mu}, 0, 0, 0\right)$. Now, we determine the basic reproduction number R_0 of the proposed model as follows:

We take only the infected compartments from the system (1) and thus, we have the following infective class sub-system:

$$\frac{dI}{dt} = \frac{(1-k)\beta\,(S_1 + pS_2)\,I}{(1+\alpha I)} - (\mu + \delta_1 + \sigma)\,I, \tag{11}$$

$$\frac{dQ}{dt} = \frac{k\beta\,(S_1 + pS_2)\,I}{(1+\alpha I)} - (\mu + \delta_2)\,Q + \sigma I, \tag{12}$$

$$\frac{dS_1}{dt} = (1-\psi)A - \frac{\beta S_1 I}{(1+\alpha I)} - \mu S_1, \tag{13}$$

$$\frac{dS_2}{dt} = \psi A - \frac{p\beta S_2 I}{(1+\alpha I)} - \mu S_2 + \theta R. \tag{14}$$

The RHS of the above infected sub-system can be written as $\mathcal{F} - \mathcal{V}$, where

$$\mathcal{F} = \begin{bmatrix} (1-k)\beta\,(S_1 + pS_2)\,\frac{I}{1+\alpha I} \\ k\beta\,(S_1 + pS_2)\,\frac{I}{1+\alpha I} \\ 0 \\ 0 \end{bmatrix} \text{ and } \quad \mathcal{V} = \begin{bmatrix} (\mu + \delta_1 + \sigma)\,I \\ -\sigma I + (\mu + \delta_2)\,Q \\ \frac{\beta S_1 I}{1+\alpha I} + \mu S_1 - (1-\psi)A \\ \frac{p\beta S_2 I}{1+\alpha I} + \mu S_2 - \theta R - \psi A \end{bmatrix}$$

Now, we have

$$X = \left[\frac{dI}{dt}, \frac{dQ}{dt}, \frac{dS_1}{dt}, \frac{dS_2}{dt}\right]$$

Let us define $F = \left[\frac{\partial(\mathcal{F})_i}{\partial x_j}\right]$ and $V = \left[\frac{\partial(\mathcal{V})_i}{\partial x_j}\right]$; for $i, j = 1, 2, 3$ at the disease-free equilibrium point E_0. Thus, the values of F and V at the disease free equilibrium point $E_0\left(\frac{(1-\psi)A}{\mu}, \frac{\psi A}{\mu}, 0, 0, 0\right)$ are given by

$$F = \begin{bmatrix} (1-k)\beta\dfrac{(1-\psi+p\psi)A}{\mu} & 0 \\ k\beta\dfrac{(1-\psi+p\psi)A}{\mu} & 0 \end{bmatrix} \quad \text{and} \quad V = \begin{bmatrix} (\mu+\delta_1+\sigma) & 0 \\ -\sigma & (\mu+\delta_2) \end{bmatrix}$$

Again, by the next-generation matrix approach, the next-generation matrix of the model is given by FV^{-1} and the basic reproduction number R_0 is determined by the spectral radius ρ of FV^{-1}. Thus, we have

$$FV^{-1} = \begin{bmatrix} (1-k)\beta\dfrac{(1-\psi+p\psi)A}{\mu\,(\mu+\delta_1+\sigma)} & 0 \\ k\beta\dfrac{(1-\psi+p\psi)A}{\mu\,(\mu+\delta_1+\sigma)} & 0 \end{bmatrix} \tag{15}$$

The eigenvalues of the matrix FV^{-1} are given by

$$\begin{vmatrix} (1-k)\beta\dfrac{(1-\psi+p\psi)A}{\mu\,(\mu+\delta_1+\sigma)} - \lambda & 0 \\ k\beta\dfrac{(1-\psi+p\psi)A}{\mu\,(\mu+\delta_1+\sigma)} & 0-\lambda \end{vmatrix} = 0 \tag{16}$$

Solving eqn.(16), we get the two eigenvalues as $\lambda = 0, \dfrac{(1-k)\beta A(1-\psi+p\psi)}{\mu\,(\mu+\delta_1+\sigma)}$

The largest eigenvalue $\dfrac{(1-k)\beta A(1-\psi+p\psi)}{\mu\,(\mu+\delta_1+\sigma)}$ gives the spectral radius ρ of FV^{-1}. Hence, the basic reproduction number R_0 is given by

$$R_0 = \frac{(1-k)\beta A(1-\psi+p\psi)}{\mu\,(\mu+\delta_1+\sigma)} \tag{17}$$

4. Equilibrium Analysis

The model described by system (1) has two equilibrium points: namely, disease-free equilibrium (DFE) point $E_0 = (\frac{(1-\psi)A}{\mu}, \frac{\psi A}{\mu}, 0, 0, 0)$ and endemic equilibrium (EE) point $E^* = (S_1^*, S_2^*, I^*, Q^*, R^*)$, which satisfy the equations:

$$(1-\psi)A - \frac{\beta S_1 I}{(1+\alpha I)} - \mu S_1 = 0, \tag{18}$$

$$\psi A - \frac{p\beta S_2 I}{(1+\alpha I)} - \mu S_2 + \theta R = 0, \tag{19}$$

$$\frac{(1-k)\beta(S_1 + pS_2)I}{(1+\alpha I)} - (\mu + \delta_1 + \sigma)I = 0, \tag{20}$$

$$\frac{k\beta(S_1 + pS_2)I}{(1+\alpha I)} - (\mu + \delta_2)Q + \sigma I = 0, \tag{21}$$

$$\delta_1 I + \delta_2 Q - \mu R - \theta R = 0. \tag{22}$$

These equations on simplification give us the following values:

$$S_1^* = \frac{(1-\psi A)}{(\frac{\beta I^*}{1+\alpha I^*} + \mu)}, \tag{23}$$

$$S_2^* = \frac{1}{p}\left[\frac{(\mu + \delta_1 + \sigma)(1+\alpha I^*)}{\beta(1-k)} - \frac{(1-\psi)A}{(\frac{\beta I^*}{1+\alpha I^*} + \mu)}\right], \tag{24}$$

$$Q^* = \frac{I^*[k(\mu + \delta_1)]}{(\mu + \delta_2)(1-k)}, \tag{25}$$

$$R^* = \left[\frac{\delta_1}{\mu + \theta} + \frac{\delta_2[K(\mu + \delta_1) + \sigma]}{(\mu + \theta)(\mu + \delta_2)(1-k)}\right] I^*. \tag{26}$$

Here, the value of I^* is given by the following quadratic equation

$$UI^{*2} + VI^* + W = 0 \tag{27}$$

where

$$U = [\delta_1(1-k)(\mu + \delta_2) + \delta_2(k(\mu + \delta_1 + \sigma) + \sigma(1-k))](\beta + a\mu)\theta p\beta$$

$$V = (\mu + \theta)(\mu + \delta_2)(\beta + a\mu)[\psi A p\beta(1-k) - (\mu + \delta_1 + \sigma)(\mu + p\beta(1-k))] +$$
$$A\beta(1-k)(1-\psi)(\mu + \theta)(\mu + \delta_2)[\alpha\mu + p\beta] + \mu\beta(1-k)(\alpha\delta_1(\mu + \delta_2) + \delta_2\theta\sigma p)$$

$$W = \mu^2(\mu + \delta_1 + \sigma)(\mu + \theta)(\mu + \delta_2)\left[R_0 - \frac{p\beta(1-k)}{\mu}\right] - \mu(\mu + \theta + \sigma)(\mu + \delta_2)$$

A solution I^* of eqn.(27) corresponds to the endemic equilibrium solution, and it is easy to observe that the system has a unique positive endemic solution by Descartes sign rule, if the following conditions hold:

(i)$R_0 > 1$, (ii)$\dfrac{\psi A p\beta(1-k)}{(\mu+\delta_1+\sigma)} > \mu + p\beta(1-k)$, (iii) $R_0 < \dfrac{p\beta(1-k)}{\mu}$.

5. Stability Analysis of Equilibrium Points

The Jacobian matrix of the system of eqns.(1) is given by

$$J(E) = \begin{bmatrix} \frac{-\beta I}{1+aI} - \mu & 0 & \frac{-\beta S_1}{(1+aI)^2} & 0 & 0 \\ 0 & \frac{-p\beta I}{(1+aI)} - \mu & \frac{-p\beta S_2}{(1+aI)^2} & 0 & \theta \\ \frac{(1-k)\beta I}{1+aI} & \frac{(1-k)p\beta I}{1+aI} & \frac{(1-k)\beta(S_1+pS_2)}{(1+aI)^2} - c & 0 & 0 \\ \frac{k\beta I}{1+aI} & \frac{kp\beta I}{1+aI} & \frac{(1-k)\beta(S_1+pS_2)}{(1+aI)^2} + \sigma & -(\mu+\delta_2) & 0 \\ 0 & 0 & \delta_1 & \delta_2 & -(\mu+\theta) \end{bmatrix} \tag{28}$$

where $c = (\mu + \delta_1 + \sigma)$.

5.1. Local Stability of Disease Free Equilibrium(DFE) Point E_0

To discuss the stability of the system at DFE point $E_0\left(\frac{(1-\psi)A}{\mu}, \frac{\psi A}{\mu}, 0, 0, 0\right)$, we have the following theorem:

Theorem *If $R_0 < 0$, then the system at the disease-free equilibrium point E_0 is locally asymptotically stable and if $R_0 > 0$, then it is unstable.*

Proof. To discuss the local stability of the system at $E_0\left(\frac{(1-\psi)A}{\mu}, \frac{\psi A}{\mu}, 0, 0, 0\right)$, we write the Jacobian matrix at E_0 as follows:

$$J(E_0) = \begin{bmatrix} -\mu & 0 & \frac{-\beta(1-\psi)A}{\mu} & 0 & 0 \\ 0 & -\mu & \frac{-p\beta\psi A}{\mu} & 0 & \theta \\ 0 & 0 & \frac{(1-k)\beta[(1-\psi)A+p\psi A]}{\mu} - c & 0 & 0 \\ 0 & 0 & \frac{k\beta[(1-\psi)A+p\psi A]}{\mu} + \sigma & -(\mu+\delta_2) & 0 \\ 0 & 0 & \delta_1 & \delta_2 & -(\mu+\theta) \end{bmatrix} \tag{29}$$

The eigenvalues are determined by $|J(E_0) - \lambda I| = 0$ and are given as: $\lambda_1 = -\mu$, $\lambda_2 = -\mu$, $\lambda_3 = -(\mu + \delta_1 + \sigma)[1 - R_0]$, $\lambda_4 = -(\mu + \delta_2)$, $\lambda_5 = -(\mu + \theta)$.
From these,we see that the four eigenvalues $\lambda_1, \lambda_2, \lambda_4$ and λ_5 of the Jacobian matrix at E_0 are negative and the remaining one eigenvalue λ_3 has negative real parts if $R_0 < 1$. Hence, the disease-free equilibrium point is locally asymptotically stable if $R_0 < 1$ and unstable if $R_0 > 1$.

5.2. Local Stability of Endemic Equilibrium Point E^*

To discuss the local stability of the system at the endemic equilibrium point $E^*\left(S_1^*, S_2^*, I^*, Q^*, R^*\right)$, we write the Jacobian matrix at E^* as follows:

$$J(E^*) = \begin{bmatrix} \frac{-\beta I^*}{1+\alpha I^*} - \mu & 0 & \frac{-\beta S_1^*}{\left(1+\alpha I^*\right)^2} & 0 & 0 \\ 0 & \frac{-p\beta I^*}{(1+\alpha I^*)} - \mu & \frac{-p\beta S_2}{\left(1+\alpha I^*\right)^2} & 0 & \theta \\ \frac{(1-k)\beta I^*}{1+\alpha I^*} & \frac{(1-k)p\beta I^*}{1+\alpha I^*} & \frac{(1-k)\beta\left(S_1^*+pS_2^*\right)}{\left(1+\alpha I^2\right)^2} - c & 0 & 0 \\ \frac{k\beta I^*}{1+\alpha I^*} & \frac{kp\beta I^*}{1+\alpha I^*} & \frac{(1-k)\beta\left(S_1^*+pS_2^*\right)}{\left(1+\alpha I^*\right)^2} + \sigma & -(\mu+\delta_2) & 0 \\ 0 & 0 & \delta_1 & \delta_2 & -(\mu+\theta) \end{bmatrix} \tag{30}$$

where $c = (\mu + \delta_1 + \sigma)$. Equation (30) can also be put in the following form:

$$J\left(E^*\right) = \begin{bmatrix} A_{11} & 0 & A_{13} & 0 & 0 \\ 0 & A_{22} & A_{23} & 0 & A_{25} \\ A_{31} & A_{32} & A_{33} & 0 & 0 \\ A_{41} & A_{42} & A_{43} & A_{44} & 0 \\ 0 & 0 & A_{53} & A_{54} & A_{55} \end{bmatrix}$$

where

$A_{11} = -\left(\frac{\beta I^*}{1+\alpha I^*} + \mu\right), \quad A_{13} = -\left(\frac{\beta S_1^*}{(1+\alpha I^*)^2}\right), \quad A_{22} = -\left(\frac{p\beta I^*}{(1+\alpha I^*)} + \mu\right),$

$A_{23} = -\left(\frac{p\beta S_2^*}{(1+\alpha I^*)^2}\right), \quad A_{25} = \theta, \ A_{31} = \frac{(1-k)\beta I^*}{1+\alpha I^*}, \quad A_{32} = \frac{(1-k)p\beta I^*}{1+\alpha I^*},$

$A_{33} = \frac{(1-k)\beta\left(S_1^*+S_2^*p\right)}{(1+\alpha I^*)^2} - c, \ A_{41} = \frac{k\beta I^*}{1+\alpha I^*}, A_{42} = \frac{kp\beta I^*}{1+\alpha I^*}, A_{43} = \frac{(1-k)\beta\left(S_1^*+S_2^*p\right)}{(1+\alpha I^*)^2} + \sigma,$

$A_{44} = -(\mu + \delta_2), A_{53} = \delta_1, A_{54} = \delta_2, A_{55} = -(\mu + \theta).$

The characteristic equation of above matrix $J\left(E^*\right)$ is given by

$$\left|J\left(E^*\right) - \lambda I\right| = \begin{vmatrix} A_{11}-\lambda & 0 & A_{13} & 0 & 0 \\ 0 & A_{22}-\lambda & A_{23} & 0 & A_{25} \\ A_{31} & A_{32} & A_{33}-\lambda & 0 & 0 \\ A_{41} & A_{42} & A_{43} & A_{44}-\lambda & 0 \\ 0 & 0 & A_{53} & A_{54} & A_{55}-\lambda \end{vmatrix} = 0$$

or $$\left|J^* - \lambda I\right| = \lambda^5 + H_1\lambda^4 + H_2\lambda^3 + H_3\lambda^2 + H_4\lambda + H_5 = 0$$

where

$H_1 = -(A_{11} + A_{22} + A_{33} + A_{44} + A_{55}),$

$H_2 = A_{11}(A_{22}+A_{44}+A_{55})+A_{13}(A_{11}-A_{31})+A_{22}(A_{33}+A_{44}+A_{55}-A_{32})+A_{33}(A_{44}+A_{55})+A_{44}A_{55}$,
$H_3 = A_{11}(-A_{55}A_{44}-A_{55}A_{22}-A_{55}A_{33}-A_{44}A_{22}-A_{44}A_{33}-A_{22}A_{33})+A_{32}(A_{25}A_{53}-A_{11}A_{23}-A_{55}A_{23}-A_{44}A_{23})+A_{55}(A_{44}A_{22}+A_{44}A_{33}+A_{22}A_{33}-A_{13}A_{31})-A_{13}(A_{55}A_{31}+A_{44}A_{31})+A_{22}A_{33}A_{44}+A_{25}A_{42}A_{54}$,
$H_4 = A_{11}(-A_{25}A_{32}A_{53}+A_{25}A_{42}A_{54}+A_{55}A_{44}A_{22}+A_{55}A_{44}A_{33}+A_{55}A_{22}A_{33}+A_{22}A_{33}A_{44}-A_{55}A_{23}A_{32}-A_{44}A_{23}A_{32})+A_{25}(A_{32}A_{53}A_{44}+A_{33}A_{42}A_{54}-A_{32}A_{43}A_{54})+A_{55}A_{44}(A_{22}A_{33}-A_{23}A_{32}-A_{13}A_{31})-A_{13}A_{31}(A_{22}A_{55}+A_{22}A_{44}+A_{55}A_{44})$,
$H_5 = A_{11}A_{25}(-A_{32}A_{53}A_{44}-A_{33}A_{42}A_{54}-A_{32}A_{43}A_{54})+A_{11}A_{55}(A_{44}A_{22}A_{33}-A_{44}A_{23}A_{32})+A_{13}(A_{25}A_{54}A_{32}A_{41}-A_{25}A_{54}A_{31}A_{42}-A_{31}A_{22}A_{55}A_{44})$.
with the following conditions:

$$H_1 > 0, H_2 > 0, H_3 > 0, H_4 > 0, H_5 > 0, H_1H_2H_3 - H_3^2 - H_1^2H_4 > 0 \text{ and,}$$
$$(H_1H_4 - H_5)\left(H_1H_2H_3 - H_3^2 - H_1^2H_4\right) - H_5\left(H_1H_2 - H_3\right)^2 - \left(H_1H_5^2\right) > 0$$

Using the Routh-Hurwitz criterion, all the eigenvalues of the Jacobian matrix have negative real parts. Thus, the endemic equilibrium point is locally asymptotically stable.

6. Sensitivity Analysis

The purpose of sensitivity analysis is to identify the sensitive parameters and to estimate these parameters with sufficient care. For the purpose, first of all, we define the sensitivity index of R_0 w.r.t. a parameter c as follows:

$S_c^{R_0} = \frac{c}{R_0}\frac{\partial R_0}{\partial c}$, where $R_0 = \frac{(1-k)\beta A(1-\psi+p\psi)}{\mu(\mu+\delta_1+\sigma)}$.

The sensitivity indices show how the model behaves with small change in any parameter value according to the above definition. The sensitivity indices of R_0 for model parameters are computed and are given in Table 2.

Table 2: Sensitivity Indices of R_0 for Model Parameters

Parameter	Sensitivity Index
A	+1
β	+1
k	−0.11111
p	+0.00008
μ	−1.11627
ψ	−0.00002
δ_1	−0.87209
σ	−0.01162

The sensitivity analysis of the model reveals that the contact rate β, and the recruitment rate A have a high positive impact on the spread of the epidemic. The parameters $\mu, \psi, \delta_1, \sigma$ have negative impact.A graphical representation of sensitivity indices of R_0 is shown in Figure 2.

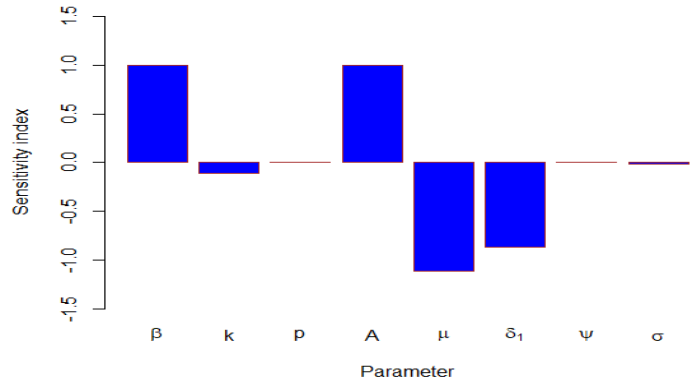

Figure 2: Graph Showing Sensitivity Indices of R_0

7. Bifurcation Analysis

The nature of the solution of a system of non-linear differential equations can be effectively described by using bifurcation analysis. In bifurcation analysis, we shall investigate the local analysis of disease-free equilibrium at $R_0 = 1$ and find the bifurcation direction. Bifurcation happens when a parameter change affects the stability of the equilibrium point.

For the analysis,let us consider $\beta = \beta^*$ as a bifurcation parameter at $R_0 = 1$, therefore, we have

$$\beta^* = \frac{\mu\left(\mu + \delta_1 + \sigma\right)}{(1-k)(1-\psi+p\psi)A}$$

Using β^* and disease-free equilibrium point E_0 in the Jacobian matrix corresponding to the system of non-linear differential equations, we have

$$J\left(\beta^*\right) = \begin{bmatrix} -\mu & 0 & \frac{(\mu+\delta_1+\sigma)(1-\psi)}{(1-k)(1-\psi+p\psi)} & 0 & 0 \\ 0 & -\mu & \frac{p(\mu+\delta_1+\sigma)\psi}{(1-k)(1-\psi+p\psi)} & 0 & \theta \\ 0 & 0 & 0 & 0 & 0 \\ 0 & 0 & \frac{k(\mu+\delta_1+\sigma)}{(1-k)} + \sigma & -\left(\mu+\delta_2\right) & 0 \\ 0 & 0 & \delta_1 & \delta_2 & -(\mu+\theta) \end{bmatrix}$$

This matrix has an eigenvalue zero at $R_0 = 1$, which is a simple eigenvalue, and all the remaining eigenvalues other than 0 are negative. Now, we apply the centre manifold theory to analyze the system as follows:
The right eigenvector corresponding to the eigenvalue zero is given by
$\left[\frac{(\mu+\delta_1+\sigma)(1-\psi)}{\mu(1-k)(1-\psi+p\psi)}, \frac{1}{\mu}\left\{\frac{p(\mu+\delta_1+\sigma)}{\mu(1-k)(1-\psi+p\psi)} + \frac{\theta}{(\mu+\theta)}\left(\delta_1 + \frac{\delta_2 k(\mu+\delta_1+\sigma)}{(1-k)(\mu+\delta_2)} + \frac{\sigma\delta_2}{(\mu+\delta_2)}\right)\right\}, 1,\right.$

$\left.\frac{1}{(\mu+\delta_2)}\left(\frac{k(\mu+\delta_1+\sigma)}{(1-k)} + \sigma\right), \frac{1}{(\mu+\theta)}\left(\delta_1 + \frac{\delta_2 k(\mu+\delta_1+\sigma)}{(1-k)(\mu+\delta_2)} + \frac{\sigma\delta_2}{(\mu+\delta_2)}\right)\right]^T$
The left eigenvector corresponding to the eigenvalue zero is $[0, 0, 1, 0, 0]$.
Using center manifold theory, we find

$$a^* = \frac{2\left(\mu+\delta_1+\sigma\right)(1-\psi)\beta}{\mu(1-\psi+p\psi)} - \frac{2\alpha\beta(1-k)A(1-\psi+p\psi)}{\mu} + \frac{2\beta p(1-k)}{\mu}$$

$$\left\{\frac{p\left(\mu+\delta_1+\sigma\right)}{(1-k)(1-\psi+p\psi)} + \frac{\theta}{(\mu+\theta)}\left(\delta_1 + \frac{\delta_2 k\left(\mu+\delta_1+\sigma\right)}{(1-k)\left(\mu+\delta_2\right)} + \frac{\delta_2\sigma}{(\mu+\delta_2)}\right)\right\}$$

and

$$b^* = \frac{(1-k)A(1-\psi+p\psi)}{\mu} > 0$$

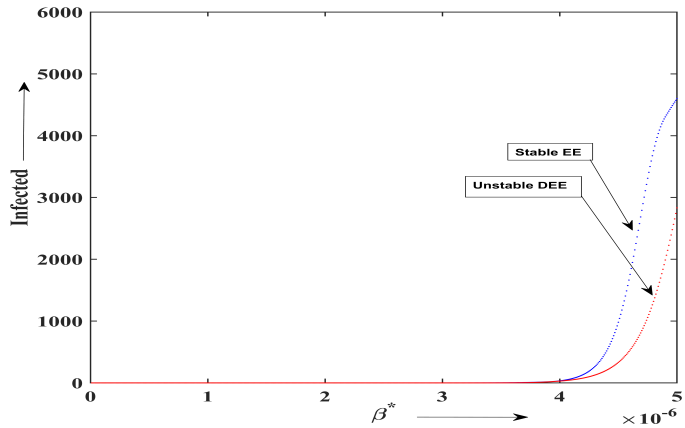

Figure 3: Graph Showing Backward Bifurcation at $R_0 = 1$

Clearly, we can see that $a^* > 0$ and $b^* > 0$ and,therefore, a backward bifurcation occurs at $R_0 = 1$ in our model which can be seen in Figure 3. This implies that the disease will exist in the population even if $R_0 < 1$.

8. Numerical Simulation

Here, we shall discuss the quantitative behaviour of infectious disease transmission dynamics. The conditions for local and global stability are determined. Now, to see the dynamic behaviour of a system of eqns.(1) using MATLAB software, we justify the analytical conclusions of the impact of infectious disease on the population.

For a disease-free equilibrium point, we use the following set of parameters: $A = 1000; \alpha = 0.00003; p = 0.8; \beta = 0.000003;\ k = 0.1; \mu = 0.02; \delta_1 = 0.15; \delta_2 = 0.01; \sigma = 0.002; \theta = 0.4; \psi = 0.0001$.

For the above set of parameters, we obtain the disease-free equilibrium point $E_0 = (49993, 5, 0, 0, 0)$ and basic reproduction number $R_0 = 0.7849$.

Similarly, for the endemic equilibrium point, we used the following set of parameter values: $A = 1000; \alpha = 0.00003; p = 0.8; \beta = 0.00001;\ k = 0.1; \mu = 0.02; \delta_1 = 0.15; \delta_2 = 0.01; \sigma = 0.002; \theta = 0.4; \psi = 0.0001$.

For the above set of parameter values, we obtain the endemic equilibrium point $E^* = (10160, 18535, 10253, 7215, 3835)$ and basic reproduction number $R_0 = 2.6162$.

Various time-series graphs are plotted by taking variations of different classes of population in Figures (4)-(9).

Figure 4(a) depicts that for different initial values of high risk of susceptible population (S_1), low risk of susceptible population (S_2), and infected population (I), the trajectories converge to disease-free equilibrium points. Hence, the disease-free equilibrium point is globally asymptotically stable in space ($S_1 - S_2 - I$).

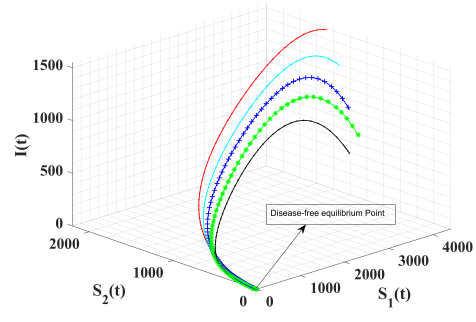

(a) Global Stability of Disease-free equilibrium point in $S_1 - S_2 - I$ space

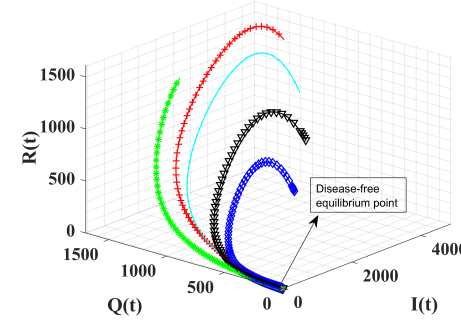

(b) Global Stability of Disease-free equilibrium point in I-Q-R space

Figure 4: **Global Stability of DFE in Different Spaces**

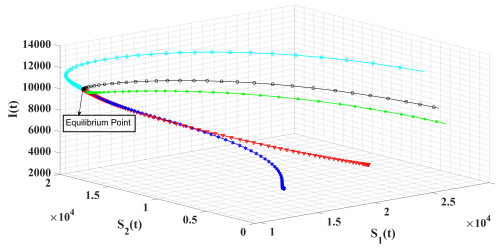

(a) Global Stability of Endemic equilibrium point in $S_1 - S_2 - I$ space

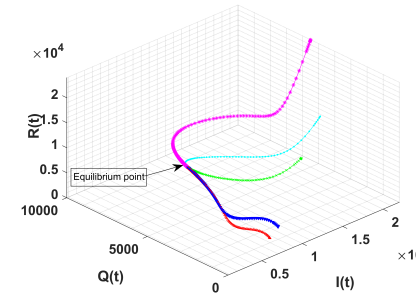

(b) Global Stability of Endemic equilibrium point in I-Q-R space

Figure 5: **Global Stability of EE in Different Spaces**

Figure 4(b) depicts that for different initial values of the infected population (I), quarantined population (Q), and recovered population (R), the trajectories converge to the disease-free equilibrium point. Hence, the disease-free equilibrium points are globally asymptotically stable in space (I-Q-R).

Figure 5(a) depicts the variation of different initial values of the high-risk susceptible population (S_1), low-risk susceptible population (S_2), and infected population (I), where the trajectories converge to an endemic equilibrium point. Hence, the endemic equilibrium point is globally asymptotically stable in space $S_1 - S_2 - I$. Figure 5(b) shows the variation of different initial values of the infected population (I), quarantined population (Q), and recovered population (R) where the trajectories converge to an endemic equilibrium point. Hence, the endemic equilibrium point is globally asymptotically stable in space (I-Q-R).

In Figure 6(a), a variation of the population in different compartments with time for various parameter values is drawn. In this figure, the variation of population in all the classes with time is shown. It is found that high-risk susceptible population (S_1) first increases with time and after some time it decreases and then reaches their respective equilibrium position. Low-risk susceptible population (S_2) increases with time and then reaches their respective equilibrium position.

From Figure 6(b), we observe that as we increase the value of β, the number of infections increases slowly but above a certain value of β, we find a rapid increase in the number of infections. It is inferred that number of infections highly depends on the transmission rate of the infectious disease.

From Figure 7(a), we observe that as we increase the value of σ, the infective population decreases and the number of infective populations is quarantined. Infective population rises i.e. more or more people are exposed to the disease and get

infected. In addition, we observe from the graph that if none of the quarantined strategies are adopted in the system, the endemic equilibrium level of the infective population rises. The impact of the saturation constant of incidence rate on the number of infections produced is shown in Figure 7(b). We observe that for less value of the saturation constant, we get higher values of infections and as we increase the value of the saturation constant, we get less number of infections.

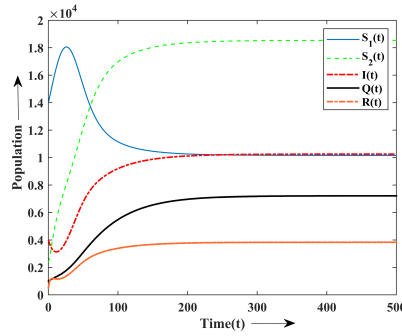

(a) Variation of Total Population with Time

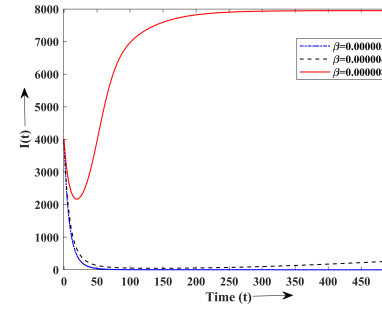

(b) Variation of Infected Population for Different Values of β

Figure 6: **Variation of the Total Population with Time and Variation of the Infected Population with Different Values of β**

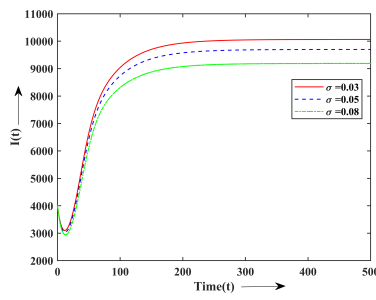

(a) Variation of Infected Population for Different Values of σ

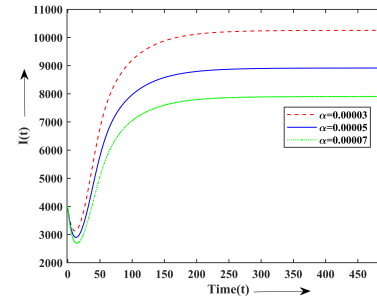

(b) Variation of Infected Population for Different Values of α

Figure 7: **Variation of Infected Population for Different Values of σ and α**

In Figure 8(a), the impact of the saturation constant of incident rate on the number of quarantined populations is shown. From this figure, we observe that for

less value of saturation constant(α), we get higher values of quarantined population and as we increase the value of saturation constant, we get less number of infections and this shows that quarantined population decreases.
From Figure 8(b), we observe that if we increase the value of the transmission coefficient (β) in the population, the number of quarantined populations increases slowly, but above a certain value of transmission coefficient (β), we find a rapid increase in the number of quarantined populations.

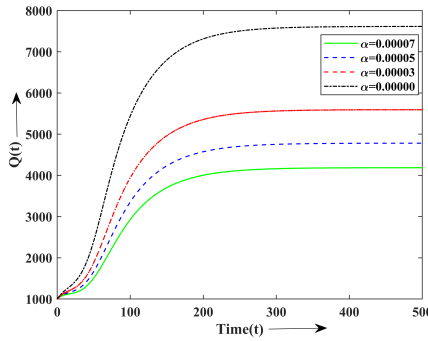

(a) Variation of Quarantine Population for Different Values of α.

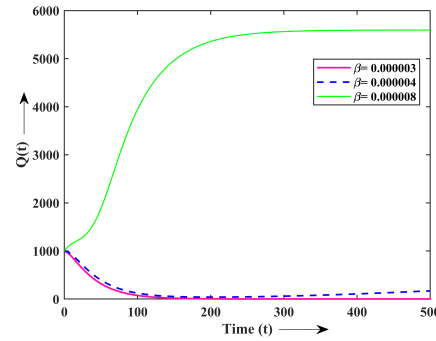

(b) Variation of Quarantine Population for Different Values of β.

Figure 8: **Variation of Quarantine Population for Different Values of α and β**

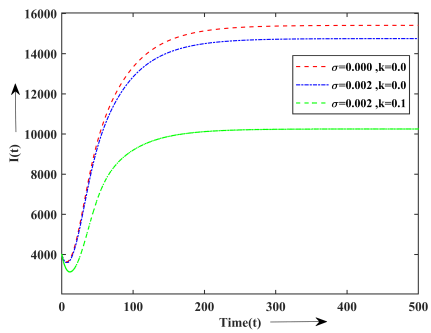

(a) Variation of Infected Population for Different Values of σ and k.

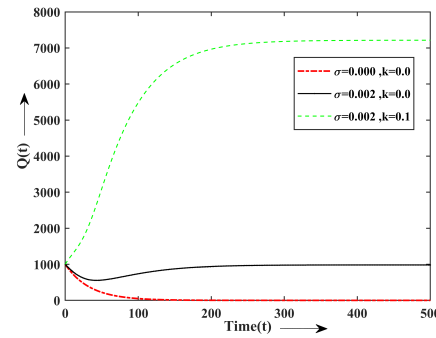

(b) Variation of Quarantine Population for Different Values of σ and k.

Figure 9: **Variation of Infected and Quarantined Population for Different Values of σ and k**

Figure 9(a) shows variation in infectious disease population with time for the different rates at which they are detected(k) and the rate at which they are quar-

antined (σ). It is observed from the figure that if control strategies such as contact tracing and quarantine are adopted in the system, then the number of infective individuals can be reduced. Further, it is found that if the infected population is not quarantined, the infective population rises i.e. more and more people are exposed to the disease and get infections. In addition, we observe from the graph that if none of the control strategies is adopted in the system, the endemic equilibrium level of the infective population rises. Figure 9(b) shows variation in infectious disease population with time for a different rate (k) at which they are detected and the rate at which they are quarantined(σ). It is observed from the figure that if control strategies (contact tracing and quarantine) are adopted in the system, then the number of quarantined populations can be increased. In addition, we observe from the graph that if none of the control strategies is adopted in the system, then the quarantined population decreases.

9. Conclusion

In this paper, a compartmental model has been proposed and analysed to investigate the impact of contact tracing and quarantine on the spread of any emerging or re-emerging epidemic by taking into account five compartments as stated earlier. We have computed the basic reproduction number R_0 for the model, which is a measure of the ability of a disease to spread infection in the population, which is found to be $R_0 = 2.6162$. We have performed a sensitivity analysis of the model to identify the significant parameters affecting the basic reproduction number. We have observed that β, A, μ and δ_1 are the significant parameters. We have also performed the bifurcation analysis and shown the co-existence of a disease-free equilibrium point with the endemic equilibrium point at $R_0 = 1$. Numerical simulations have been performed to observe the effects of contact tracing and quarantine strategies in reducing the spread of the epidemic. The disease-free equilibrium point is shown to be locally asymptotically stable when $R_0 < 1$ and unstable when $R_0 > 1$. Time series graphs have been plotted to study the effect of various effective parameters on the system with respect to time. A numerical investigation of the model shows that contact tracing and quarantine play a key role in controlling the diseases. Our study shows that contact tracing and quarantine strategies are effective intervention measures to reduce the disease burden on the population.

In the future, we can incorporate the fuzzy concept to understand the uncertainty or ambiguity in recognising low-risk and high-risk susceptibles.

Acknowledgement

The authors are grateful to referees for their careful reading, valuable comments, and making helpful suggestions to improve the paper.

References

[1] Agarwal M. and Bhadauria Archana S., Modeling H1N1 flu epidemic with contact tracing and quarantine, International Journal of Biomathematics, 5(05) (2012), 1250038.

[2] Aparicio J. Pablo, Julio C. Hernández, Preventive treatment of tuberculosis through contact tracing, Contemporary Mathematics, 410 (2006), 17-30.

[3] Biala T. A., Afolabi Y. O., Khaliq A. Q. M., How efficient is contact tracing in mitigating the spread of COVID-19? a mathematical modeling approach, Applied mathematical modelling, 103 (2022), 714-730.

[4] Brauer F., Carlos Castillo-Chavez, Mathematical models in population biology and epidemiology, 2 (2012).

[5] Capasso V., Mathematical structures of epidemic systems, Springer Science and Business Media, 97 (2008).

[6] Capasso V., Gabriella Serio, A generalization of the Kermack-McKendrick deterministic epidemic model, Mathematical biosciences, 42(1-2) (1978), 43-61.

[7] Castillo-Chavez, Carlos, Baojun Song, Dynamical models of tuberculosis and their applications, Math. Biosci. Eng, 1(2) (2004), 361-404.

[8] Chinviriyasit, Settapat, Wirawan C., Global stability of an SIQ epidemic model, Agriculture and Natural Resources, 41(5) (2007), 225-228.

[9] Diekmann O., Johan Andre Peter Heesterbeek, Johan AJ Metz, On the definition and the computation of the basic reproduction ratio R 0 in models for infectious diseases in heterogeneous populations, Journal of mathematical biology, 28 (1990), 365-382.

[10] Driessche V., Pauline, Reproduction numbers of infectious disease models, Infectious disease modelling, 2, No. 3 (2017), 288-303.

[11] Eames Ken TD, Matt J. Keeling, Contact tracing and disease control, Proceedings of the Royal Society of London, Series B: Biological Sciences, 270 (1533) (2003), 2565-2571.

[12] Garba Salisu Mohammed, Abba B. Gumel, MR Abu Bakar, Backward bifurcations in dengue transmission dynamics, Mathematical biosciences, 215(1) (2008), 11-25.

[13] Goudiaby M. S., Gning L. D., Diagne M. L., Dia Ben M., Rwezaura H., J. Tchuenche M., Optimal control analysis of a COVID-19 and tuberculosis co-dynamics model, Informatics in Medicine Unlocked, 28 (2022), 100849.

[14] Herbert H., Zhien Ma, Shengbing Liao, Effects of quarantine in six endemic models for infectious diseases, Mathematical biosciences, 180(1-2) (2002), 141-160.

[15] Herbert Hethcote W., The mathematics of infectious diseases, SIAM review, 42(4) (2000), 599-653.

[16] Hu Z., Yang Y., Wanbiao M., The Analysis of Two Epidemic Models with Constant Immigration and Quarantine, The Rocky Mountain Journal of Mathematics, (2008), 1421-1436.

[17] Izadi, M., Waezizadeh, T., Stability analysis and numerical evaluations of a COVID-19 model with vaccination, BMC Medical Research Methodology, 24(1) (2024), 97.

[18] Kunwar L. B., Verma V. S., Mathematical Analysis of SVEIQR Model for COVID-19, South East Asian Journal of Mathematics and Mathematical Sciences, 19(1) (2023).

[19] Pozo-Martin F., Beltran Sanchez M. A., Müller S. A., Diaconu V., Weil K., Bcheraoui C. El., Comparative effectiveness of contact tracing interventions in the context of the COVID-19 pandemic: a systematic review, European Journal of Epidemiology, 38(3) (2023), 243-266.

[20] Rutherford George W., Jean M. Woo., Contact tracing and the control of human immunodeficiency virus infection, JAMA, 259(24) (1988), 3609-3610.

[21] Sharma Swarnali and Samanta G. P., Stability analysis and optimal control of an epidemic model with vaccination, International Journal of Biomathematics, 8(03) (2015), 1550030.

[22] Verma V. S., Kunwar L. B., Bhadauria Archana Singh, Rana Vikash, An SVIQR Epidemic Model for COVID-19, South East Asian Journal of Mathematics and Mathematical Sciences, 18(3) (2022).

[23] Waezizadeh, T., Ebrahimi, N., Dynamical model for COVID-19 in a population, J Mahani Math Res, 11(1) (2022), 25-34.

[24] Wu F., Liang X., Lei J., Modelling COVID-19 epidemic with confirmed cases-driven contact tracing quarantine, Infectious Disease Modelling, 8(2) (2023), 415-426.

[25] Zaman G., Yong H. K., Jung I. H., Stability analysis and optimal vaccination of a SIR epidemic model, BioSystems, 93(3) (2008), 240-249.

[26] Zhenguo B., Zhou Y., Global dynamics of an SEIRS epidemic model with periodic vaccination and seasonal contact rate, Nonlinear Analysis: Real World Applications, 13(3) (2012), 1060-1068.